Supporting Information for: Diffusion equation for the longitudinal spectral diffusion: the case of the RIDME experiment

Sergei Kuzin*, Gunnar Jeschke, Maxim Yulikov*

[a] *ETH Zürich, Department of Chemistry and Applied Bioscience, Laboratory of Physical Chemistry, Vladimir-Prelog-Weg 2, 8093 Zürich, Switzerland*

Contents

1. Properties of the diffusion equation and its solution

Some straightforward remarks can be given on the $\mu(\omega, t)$ dynamics in the following two special cases:

Case $\rho(\omega) = const$: In this case there are no energetic or statistical preferences for certain states, which recalls the case of simple diffusion in a homogeneous medium. Substitution of this condition results in the conventional diffusion equation:

$$\frac{\partial \mu(\omega, t)}{\partial t} = D\rho \frac{\partial^2 \mu(\omega, t)}{\partial \omega^2}$$

Case $\mu(\omega, t_0) = \rho(\omega)$: As discussed above, this is a limiting case, where no macroscopic changes are expected, which is also satisfied by the equation.

Intensity, or bulk electron magnetisation (see Equation (9) in the main text), is conserved during the evolution with the equation under consideration which is in agreement with the picture that nuclear evolution doesn't change polarisation of electron spin.

$$\frac{d}{dt} M(t) = D \int_{-\infty}^{+\infty} (\rho \mu''_{\omega\omega} - \rho'' \mu) d\omega = 0$$

Energy, $E(t) = \int \omega \mu(\omega, t) d\omega$ is dissipated.

$$\frac{d}{dt} E(t) = -D \int_{-\infty}^{+\infty} (\rho \mu'_{\omega} - \rho' \mu) d\omega = 2D \int_{-\infty}^{+\infty} \rho' \mu(\omega, t) d\omega \qquad \text{(S1)}$$

One can derive a value that has the meaning of *energy dissipation time*. Suppose that at the moment $t = t_0$ the magnetisation spectrum can be approximated as follows

$$\mu(\omega, t_0) = \rho + \varepsilon \rho'.$$

After substitution in (S1):

$$\frac{d}{dt} E(t) = 2D \int_{-\infty}^{+\infty} \rho' \rho + \varepsilon \rho'^2 d\omega = 2D\varepsilon \int_{-\infty}^{+\infty} \rho'^2 d\omega.$$

At the same time

$$E(t_0) = \int_{-\infty}^{+\infty} \omega \rho + \varepsilon \omega \rho' d\omega = \langle E \rangle - \varepsilon$$

Where $\langle E \rangle$ is a mean energy at dynamic equilibrium of nuclear reservoir. It means that

$$\frac{d}{dt}E(t) = -\frac{E(t) - \langle E \rangle}{\tau_E}$$

$$\tau_E = \frac{1}{2D\int_{-\infty}^{+\infty} \rho'^2 d\omega}.$$

In the special case of Gaussian distribution $\rho(\omega) = \exp(-\omega^2/2\sigma^2)/\sqrt{2\pi}\sigma$ and $\tau_E = \sqrt{\pi/2}(D/\sigma^3)^{-1}$.

2. General solution of the diffusion equation

We have not found an analytical solution of equation (16). Therefore, we decided to introduce a basis set of functions and to transform the problem to a matrix equation. The main application of the developed formalism deals with a Gaussian shape of $\rho(\omega) = \exp(-\omega^2/2\sigma^2)/\sqrt{2\pi}\sigma$. Thus, the Hermitian basis set was chosen as follows ($n \geqslant 0$)

$$|e_n\rangle = He_n\left(\frac{\omega}{\sigma}\right)\rho(\omega) = \frac{1}{\sqrt{2\pi}\sigma}He_n\left(\frac{\omega}{\sigma}\right)\exp\left(-\frac{\omega^2}{2\sigma^2}\right). \tag{S2}$$

Here $He_n(x)$ are so-called *probabilists's* Hermitian polynomials:[1] $He_n(x) = (-1)^n e^{x^2/2}(e^{-x^2/2})^{(n)}$. Note that this set of functions is not unique but parameterised by spectrum width σ. A convenient representation of basis functions follows directly from the definition:

$$|e_n\rangle = (-\sigma)^n \rho^{(n)}(\omega). \tag{S3}$$

The introduced basis is not orthogonal with the canonical functional scalar product. However, Hermitian polynomials, form an orthogonal series with a weight function:

$$\int_{-\infty}^{+\infty} He_k(x)He_n(x)e^{-\frac{x^2}{2}}dx = \delta_{nk}n!\sqrt{2\pi}.$$

We represent solution as a following series with time-dependent coefficients:

$$\mu(\omega, t) = \sum_k c_k(t)He_k\left(\frac{\omega}{\sigma}\right)\rho(\omega), \tag{S4}$$

After substitution of the chosen series to the equation (16)

$$\sum_k \dot{c}_k(t) He_k\left(\frac{\omega}{\sigma}\right)\rho(\omega) = \frac{D}{\sigma^2}\sum_k c_k(t)\left[He_{k+2}\left(\frac{\omega}{\sigma}\right) - He_2\left(\frac{\omega}{\sigma}\right)He_k\left(\frac{\omega}{\sigma}\right)\right]\rho^2(\omega)$$

multiplication of both sides by $He_n(\omega/\sigma)$ followed by integration gives:

$$n!\dot{c}_n(t) = \frac{D}{\sigma^2}\sum_k c_k(t)\int_{-\infty}^{+\infty} He_n\left(\frac{\omega}{\sigma}\right) \times \left(He_{k+2}\left(\frac{\omega}{\sigma}\right) - He_2\left(\frac{\omega}{\sigma}\right)He_k\left(\frac{\omega}{\sigma}\right)\right)\rho^2(\omega)d\omega$$

This result can be reformulated in a matrix form as $\dot{\vec{c}}(t) = \frac{D}{\sigma^3}\hat{\Gamma}\vec{c}(t)$ with the time-independent matrix

$$\Gamma_{nk} = \frac{1}{n!2\pi}\int_{-\infty}^{+\infty} He_n(x)(He_{k+2}(x) - He_2(x)He_k(x))e^{-x^2}dx.$$

$$\Gamma_{nk} = \begin{cases} 0, & \text{if } n=0 \text{ or } k=0 \text{ or } n+k \text{ is odd} \\ (-1)^k \frac{nk(n+k-3)!!}{n!\sqrt{4\pi}}\left(-\frac{1}{2}\right)^{\frac{n+k}{2}-1} & \text{otherwise} \end{cases} \tag{S5}$$

In the above formula for matrix elements we let by definition $(-1)!! = 1$ to reach consistency of the expression. Finally, the solution in the chosen basis set:

$$\vec{c}(t) = e^{\frac{D}{\sigma^3}\hat{\Gamma}t}\vec{c}(0). \tag{S6}$$

The initial condition on $\mu(\omega, 0)$ is represented in the following way:

$$c_n(0) = \frac{1}{n!}\int_{-\infty}^{+\infty} He_n\left(\frac{\omega}{\sigma}\right)\mu(\omega,0)d\omega. \tag{S7}$$

3. Frequency correlation function

In this section, the expression (20) is derived. Consider the actual frequency of hyperfine interaction of an unpaired electron with nuclear spin bath as a random variable parameterised by mixing time, $\omega(T_{mix})$. Because

we can safely neglect thermal polarisation of the nuclear spin subsystem the average hyperfine frequency is zero, $\overline{\omega(T_{mix})} = 0$. One can introduce its correlation function as ensemble average $C_\omega(T_{mix}) = \overline{\omega(0)\omega(T_{mix})}$. We will calculate this function by solving the equation (16) with Dirac delta initial conditions $\mu(\omega, 0) = \delta(\omega - \omega_0)$ followed by the averaging over all possible initial frequencies ω_0. We expand this initial condition as a series with coefficients (S7):

$$c_n(0;\omega_0) = \frac{1}{n!}\int_{-\infty}^{+\infty} \delta(\omega-\omega_0) He_n\left(\frac{\omega}{\sigma}\right) d\omega = \frac{1}{n!} He_n\left(\frac{\omega_0}{\sigma}\right)$$

For the ensemble under consideration the correlation function turns to $\omega_0 \cdot \overline{\omega(T_{mix})} = \omega_0 \int \omega\mu(\omega, T_{mix})d\omega$. We notice then

$$\begin{aligned}\overline{\omega(T_{mix})} &= \int_{-\infty}^{+\infty} \omega \sum_k c_k(T_{mix};\omega_0) He_k\left(\frac{\omega}{\sigma}\right)\rho(\omega)d\omega \\ &= \sum_k c_k(T_{mix};\omega_0)\frac{\sigma}{\sqrt{2\pi}}\int_{-\infty}^{+\infty} He_1(x)He_k(x)e^{-\frac{x^2}{2}}dx \\ &= \sigma c_1(T_{mix};\omega_0) = \sigma\cdot\left(e^{\frac{D}{\sigma^3}T_{mix}\hat{\Gamma}}\vec{c}(0;\omega_0)\right)_1.\end{aligned}$$

Here we used the observation that $\omega = \sigma\cdot He_1(\omega/\sigma)$ and, in addition, orthogonality of Hermitian polynomials. Subscript '1' means the first component of the resulting column (note that elements numeration starts with 0). After averaging over all starting frequencies with weighting function $\rho(\omega_0)$ we have

$$\begin{aligned}C_\omega(T_{mix}) &= \int_{-\infty}^{+\infty} \omega_0\overline{\omega(T_{mix})}\rho(\omega_0)d\omega_0 \\ &= \sigma\left(e^{\frac{D}{\sigma^3}\hat{\Gamma}T_{mix}}\int_{-\infty}^{+\infty}\omega_0\vec{c}(0;\omega_0)\rho(\omega_0)d\omega_0\right)_1\end{aligned}$$

As a last step we find that

$$\int_{-\infty}^{+\infty}\omega_0 c_k(0;\omega_0)\rho(\omega_0)d\omega_0 = \frac{\sigma}{\sqrt{2\pi}k!}\int_{-\infty}^{+\infty} He_1(x)He_k(x)e^{-\frac{x^2}{2}}dx = \sigma\delta_{1,k}$$

with the Kronecker symbol $\delta_{m,n}$. This leads us to the final expression

$$C_\omega(T_{mix}) = \sigma^2\left(e^{\frac{D}{\sigma^3}\hat{\Gamma}T_{mix}}\right)_{1,1}.$$

4. Derivation of *ih*-RIDME signal

The pulse sequence of 5-pulse RIDME is given in the main text Figure 1b. This experiment was designed by Milikisyants *et al.*[2] as a dead-time-free version of the originally suggested 3-pulse RIDME experiment of Kulik *et al.*[3] (Figure 1c). The first two pulses of the 5-pulse RIDME pulse sequence, separated by delay d_1, form a primary echo (PE) where ideally all interactions are refocused. The described step allows in practice moving the so-called mixing block (pulses 3 and 4) arbitrarily close to the PE and even making a full overlap with it. In the approximation of ideally refocused interactions (or, equivalently, dropping all non-secular terms of the Hamiltonian) the block of the first two pulses can be replaced back by a single $\pi/2$-pulse at the position of PE. The function of the mixing block is to store the electron magnetisation in z-direction, after a $\pi/2$-pulse, where as compared to the fast transverse decay it undergoes significantly slower spin-lattice relaxation processes. During this block, the spin system state of coupled electrons and nuclei stochastically changes leading to electron dipolar modulation and to a background decay. Theoretically, the signal acquisition in the RIDME experiment can be positioned on the stimulated echo (SE) after the mixing block. In this version of the experiment though the total time of transverse evolution will increase as the mixing block shifts. Consequently, transverse relaxation has non-constant influence on the signal intensity making theoretical analysis of experimental traces more cumbersome. This is why the last π-pulse is added: it produces the so-called 'refocused virtual echo' (RVE), whose position does not change upon shift of the mixing block. If the mentioned above secular approximation is assumed for the Hamiltonian during the whole transverse part of RIDME experiment than no difference between the dependence of the SE and RVE on the timing appears. This consideration simplifies the propagation in the RIDME experiment, and makes it identical to the propagation in the original 3-pulse version (see Figure 1c). Note also our discussion on the separation of transverse and longitudinal contributions in the RIDME signal in the section 4.1.

According to conventional 5p-RIDME phase cycling[2] the phases of the mixing block's pulses are the same and vary as $+x, -x, +y, -y$. The phase alternation $+x, -x$ is for removal of any constant offset. Changing the mixing block phase between $+x$ and $+y$ allows to store different components of the magnetisation spectrum, namely, $\rho(\omega)\cos(\omega\tau)$ and $\rho(\omega)\sin(\omega\tau)$ respectively (sign is not concerned here). Table S1 summarises all the contributions to

p1	p2 and p3	$\mu_\tau(\omega,0)$	Echo intensity	Detection
$+x$	$+x$	$\rho(\omega)\cos(\omega\tau)$	$\int \mu_\tau(\omega,T_{mix})\cos(-\omega\tau)d\omega$	+
$+x$	$-x$	$-\rho(\omega)\cos(\omega\tau)$	$-\int \mu_\tau(\omega,T_{mix})\cos(-\omega\tau)d\omega$	+
$+x$	$+y$	$\rho(\omega)\sin(\omega\tau)$	$\int \mu_\tau(\omega,T_{mix})\sin(-\omega\tau)d\omega$	+
$+x$	$-y$	$-\rho(\omega)\sin(\omega\tau)$	$-\int \mu_\tau(\omega,T_{mix})\sin(-\omega\tau)d\omega$	+
$-x$	$+x$	$-\rho(\omega)\cos(\omega\tau)$	$-\int \mu_\tau(\omega,T_{mix})\cos(-\omega\tau)d\omega$	-
$-x$	$-x$	$\rho(\omega)\cos(\omega\tau)$	$\int \mu_\tau(\omega,T_{mix})\cos(-\omega\tau)d\omega$	-
$-x$	$+y$	$-\rho(\omega)\sin(\omega\tau)$	$-\int \mu_\tau(\omega,T_{mix})\sin(-\omega\tau)d\omega$	-
$-x$	$-y$	$\rho(\omega)\sin(\omega\tau)$	$\int \mu_\tau(\omega,T_{mix})\sin(-\omega\tau)d\omega$	-

Table S1: Details of the phase cycling in the *ih*-RIDME experiment. The phase of the first (p1), respectively, the second and the third (p2 and p3) $\pi/2$-pulse is given; $\mu_\tau(\omega,T_{mix})$ is the formal result of relaxation during time T_{mix} of initial magnetisation $\mu_\tau(\omega,0)$ regardless of its exact shape.

the detected RIDME signal intensity depending on particular pulse phases within the phase protocol. After following the summation one can find that the *ih*-RIDME contribution is a sum of $\int \mu_\tau(\omega,T_{mix})\cos(-\omega\tau)d\omega$ with initial condition $\mu_\tau(\omega,0)=\rho(\omega)\cos(\omega\tau)$ and of $\int \mu_\tau(\omega,T_{mix})\sin(-\omega\tau)d\omega$ with initial condition $\mu_\tau(\omega,0)=\rho(\omega)\sin(\omega\tau)$. Since the evolution equation is linear with respect to $\mu(\omega,t)$ and real i.e. doesn't mix real and imaginary part of $\mu(\omega,t)$, this sum discussed is equivalent to

$$R(\tau;T_{mix})=\Re\left[\int_{-\infty}^{+\infty} e^{-i\omega\tau}\mu_\tau(\omega,T_{mix})d\omega\right]. \tag{S8}$$

Where $\mu_\tau(\omega,T_{mix})$ is short for the result of $\mu(\omega,0)=\rho(\omega)e^{i\omega\tau}$ relaxation during time T_{mix}. Here, $\Re$ is the real part operator, and $R(\tau,T_{mix})$ is the RIDME echo signal that only accounts for the LSD (without considering proton spectral diffusion during the transverse evolution), for the mixing block of duration T_{mix} at a time τ after the primary echo. Thus, RIDME echo intensity is proportional to the real part of relaxed magnetisation spectrum's Fourier transform.

Finally, we can substitute the representation of $\mu_\tau(\omega,T_{mix})$ as a series (S4)

$$R(\tau;T_{mix})=e^{-\frac{\sigma^2\tau^2}{2}}\Re\left[\sum_k c_k^\tau(T_{mix})(-i\sigma\tau)^k\right] \tag{S9}$$

As it was shown before (see Eq. (S7))

$$c_n^{\tau}(0) = \frac{1}{\sigma n! \sqrt{2\pi}} \int_{-\infty}^{+\infty} He_n\left(\frac{\omega}{\sigma}\right) e^{-\frac{\omega^2}{2\sigma^2}} e^{i\omega\tau} d\omega = \frac{(i\sigma\tau)^n}{n!} e^{-\frac{\sigma^2\tau^2}{2}} \tag{S10}$$

5. Details on *ih*-RIDME traces numerical computation

The derived equation of the longitudinal spectral diffusion (16) includes the shape of the hyperfine spectrum $\rho(\omega)$. For an arbitrary shape, an analytical solution was not found. Instead of solving the differential equations numerically we preferred to introduce a convenient basis set and therefore transform the problem into the matrix form. For the special case of a Gaussian hyperfine spectrum the set of Hermitian functions was chosen (S2). In practical applications, this basis set needs to be truncated. The reduction of basis function may affect the computation results. The convergence of the computed RIDME data with the increase of basis set's size `dim` is shown in Figure S1. As it immediately follows from (S12), the master plot of the *ih*-RIDME background is parameterised by two dimensionless combinations $\sigma\tau$ and DT_{mix}/σ^3. In the presented example DT_{mix}/σ^3 was put equal to 0.5. For comparison, given the value of $\Delta = D/\sigma^3 = 18\ ms^{-1}$ (see Table 2), corresponding T_{mix} is ca. 30 μs.

From this Figure, one can find that the computation converges relatively quickly. To converge until the $1/e$-decay already 15 elements of the basis set are enough. In this work, the first 51 functions (`dim`=51) were chosen, which is sufficient for precise computation and does not cause any time or memory problems for modern desktop computers. On the other hand, we need to emphasise that `dim` should be chosen as small as reasonably possible. As matrix elements Γ_{nk} of the relaxation operator $\hat{\Gamma}$ (S5) grow fast for any fixed n, numerical errors may appear during matrix exponent computation. This is demonstrated by the light-blue line where the value of `dim` was deliberately overshot: `dim`=147. A quantitative demonstration is given on the right panel of Figure S1. The deviation between a reference trace (`dim` = 51) and a test trace (`dim` is varied) is calculated according to the expression:

$$\mathrm{rmsd}(\texttt{dim}) = \sqrt{\frac{1}{N_{points}} \sum_{i=1}^{N_{points}} (R(\tau_i; T_{mix}, \texttt{dim}) - R(\tau_i; T_{mix}, \texttt{dim} = 51))^2}. \tag{S11}$$

It is to observe the fast converging in the beginning, the stable region until ca. `dim`=125 and numerical instability in larger sets.

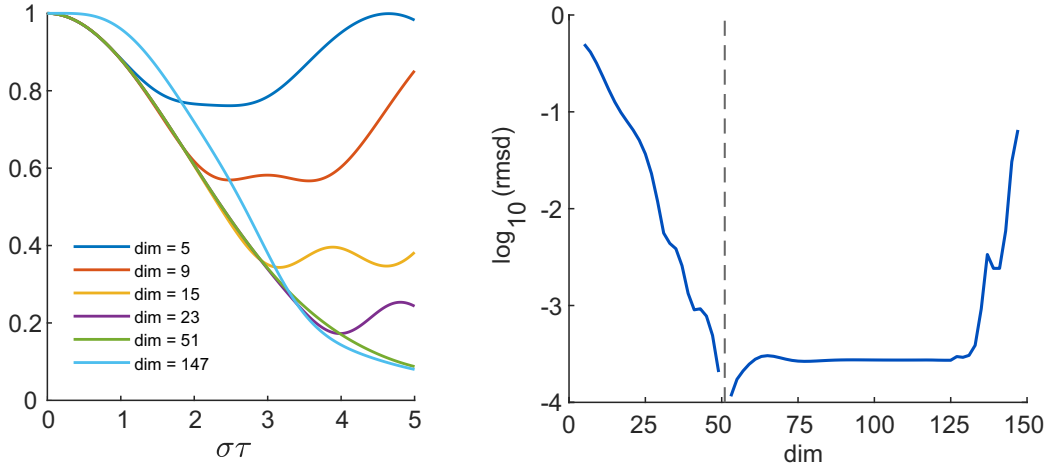

Figure S1: Left: Convergence of computed *ih*-RIDME traces, $R(\tau; T_{mix})$, with respect to various truncation of the basis set of Hermitian functions. Example is computed for $DT_{mix}/\sigma^3 = 0.5$. In this work, a basis set with 51 elements was used. Right: Computed rmsd with respect to the reference trace (`dim`=51) as a function of basis set's size.

It is also advantageous to arrange the basis set such that the even elements are grouped separately from the odd ones. This way matrix $\hat{\Gamma}$ becomes block-diagonal which makes computation of the exponent faster. Such an arrangement was, however, not implemented in our actual computations.

In the routine calculations, one more simplification of the implementation can be used. Namely, setup of the initial condition (S10) and immediate calculation of the echo intensity (S8) correspond to a solution of simple differential equation $\partial\mu/\partial t = \pm i\omega\mu$. The sign '+' is used for the evolution before the mixing block and '−' is used for the evolution after the mixing block. In the basis set (S2) this becomes a matrix operation $\partial\vec{c}/\partial t = \pm i\sigma\hat{R}\vec{c}$ with a sparse matrix $\hat{R}$:

$$(\hat{R})_{nk} = \begin{cases} -1, & \text{if } n = k+1 \\ k, & \text{if } n = k-1 \\ 0 & \text{otherwise.} \end{cases}$$

In such a formalism the computation of RIDME trace can be rewritten in a

simple form

$$R(\tau; T_{mix}) = \left(\exp(-i\sigma\hat{R}\tau)\exp(DT_{mix}/\sigma^3\hat{\Gamma})\exp(i\sigma\hat{R}\tau)\vec{c}_{init}\right)_0, \qquad \text{(S12)}$$

where $\vec{c}_{init}$ is a column vector with only its first element not equal to 0. The sub-index '0' after the brackets means that the element of the column with the index 0 needs to be taken.

6. A note on the transverse evolution

In principle, the proposed formalism can be extended to account for the spectral diffusion during the transverse evolution. This can be achieved by adding a term in (16) that describes continuous gain of phase difference of sub-ensembles with different hyperfine shifts ω

$$\frac{\partial\mu(\omega,t)}{\partial t} = i\omega\mu(\omega,t) + D\left(\rho(\omega)\frac{\partial^2\mu(\omega,t)}{\partial\omega^2} - \rho''(\omega)\mu(\omega,t)\right). \qquad \text{(S13)}$$

After numerous tries we must conclude that such a modification is not able to consistently and quantitatively reproduce purely transverse experiments (such as Hahn echo decay or Carr-Purcell experiments). Possibly, this is connected to the fact that in the transverse evolution experiments the characteristic spectral diffusion times are short and fall in the range where our model's approximations are too rough. A possible further development of the diffusion equation model would be in allowing a frequency dependence for the parameter D. It is however difficult to estimate in advance if this would lead to a significant improvement in describing the transverse evolution data.

7. Detailed samples composition

The studied solutions were prepared using the following scheme. A stock solution of TEMPO in D_2O (its mass is given in the Table S2 in the column m_S) was mixed with D_2O ($m(D_2O)$) and/or with H_2O ($m(H_2O)$). After careful stirring a portion of the mixture (m(sol)) was taken and mixed with deuterated ($m(D_8G)$) or protonated ($m(H_8G)$) glycerol. Again, the final mixture was stirred using a vortex mixer for 1 minute. All measured masses are given in the Table S2.

Sample	m_S	$m(D_2O)$	$m(H_2O)$	m(sol)	$m(D_8G)$	$m(H_8G)$
1	4.40	0	34.99	18.70	0	19.28
2	4.47	0	35.74	20.88	21.79	0
3	4.39	17.64	18.60	21.96	22.27	0
4	4.44	28.75	9.82	20.02	21.10	0
5	4.39	39.16	0	22.41	23.84	0
6	4.49	39.20	0	22.36	0	19.74

Table S2: Masses of all solvents used for samples preparation. Names of columns are explained in this section. All values are given in milligrams.

8. Relaxation data

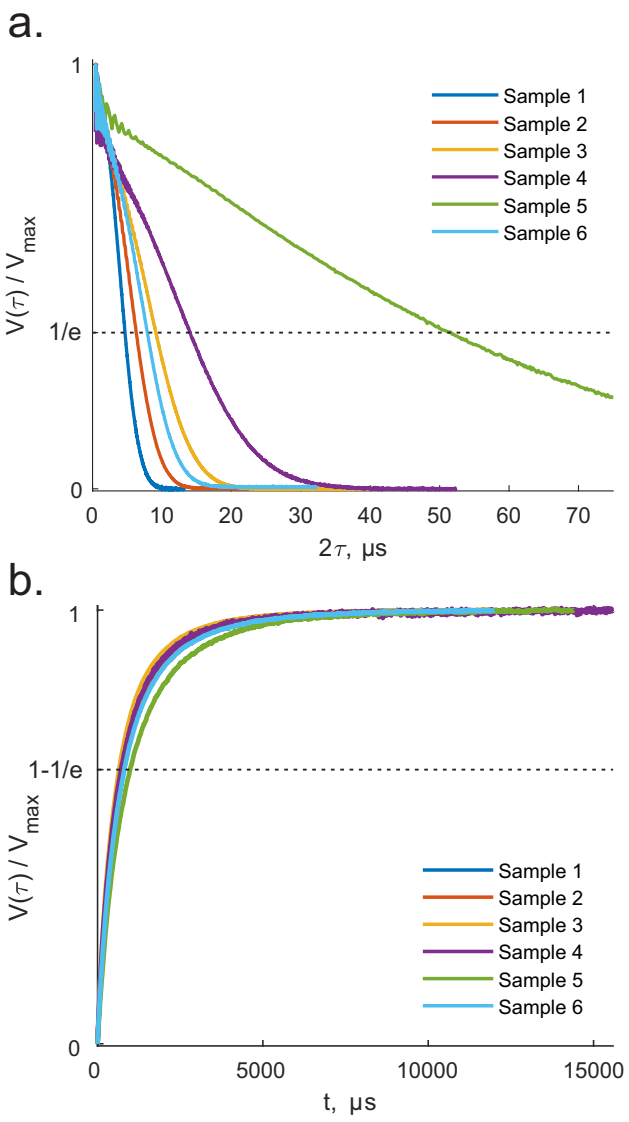

Figure S2: Normalized T_2-relaxation (a) and inversion recovery (b) traces of the samples studied in this work. Corresponding relaxation times are summarised in the Table 1 in the main text.

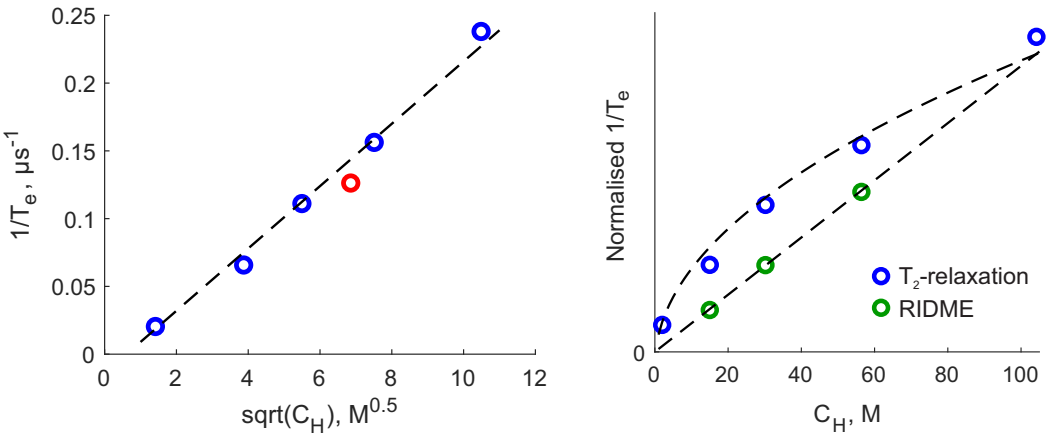

Figure S3: Left: Linearization of relaxation times T_2 as function of proton concentration (samples 1-5). Red circle corresponds to the sample 6. Right: The behaviour of characteristic times of RIDME and T_2-relaxation traces is compared. For the purpose of simplicity, the data are normalised to the maximum proton concentration in our experiments.

9. Comparison of experimental RIDME traces with different d_1-interpulse delays

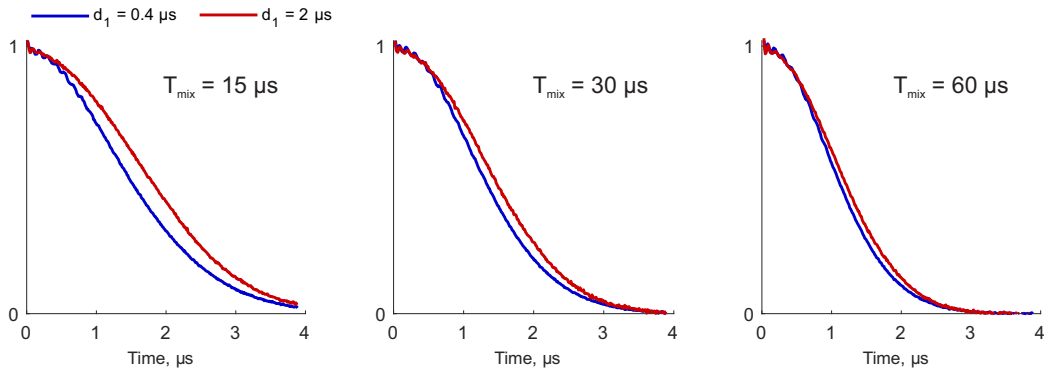

Figure S4: Comparison of RIDME traces (sample 2, see main text) with d_1 (the first interpulse delay) set to 0.4 μs (blue line) and 2 μs (red line).

10. Global fit of RIDME traces with $T_{mix}^{ref} = 15\ \mu s$

This section demonstrates that using a reference trace with a too short mixing time leads to a larger deviations of the best fit and the RIDME data. Here we show the best fits for the RIDME data divided by the trace with $T_{\mathrm{mix}} = 15\ \mu$s, while in the main text the reference trace has $T_{\mathrm{mix}} = 30\ \mu$s. The overall agreement of the fits is visibly worse here, as compared to the main text example.

Sample	Water	Glycerol	D/σ^3, ms^{-1}	σ/C_H, MHz/M
2	H	D	21.2 ± 1.6	0.0204 ± 0.0005
6	D	H	19.9 ± 1.8	0.0200 ± 0.0005

Table S3: Summary of the experimental RIDME data fitting for samples 2 and 6. Reference mixing time was chosen 15 μs. Uncertainties of the parameters are given and 10%-increase of rmsd while the other parameter was fixed.

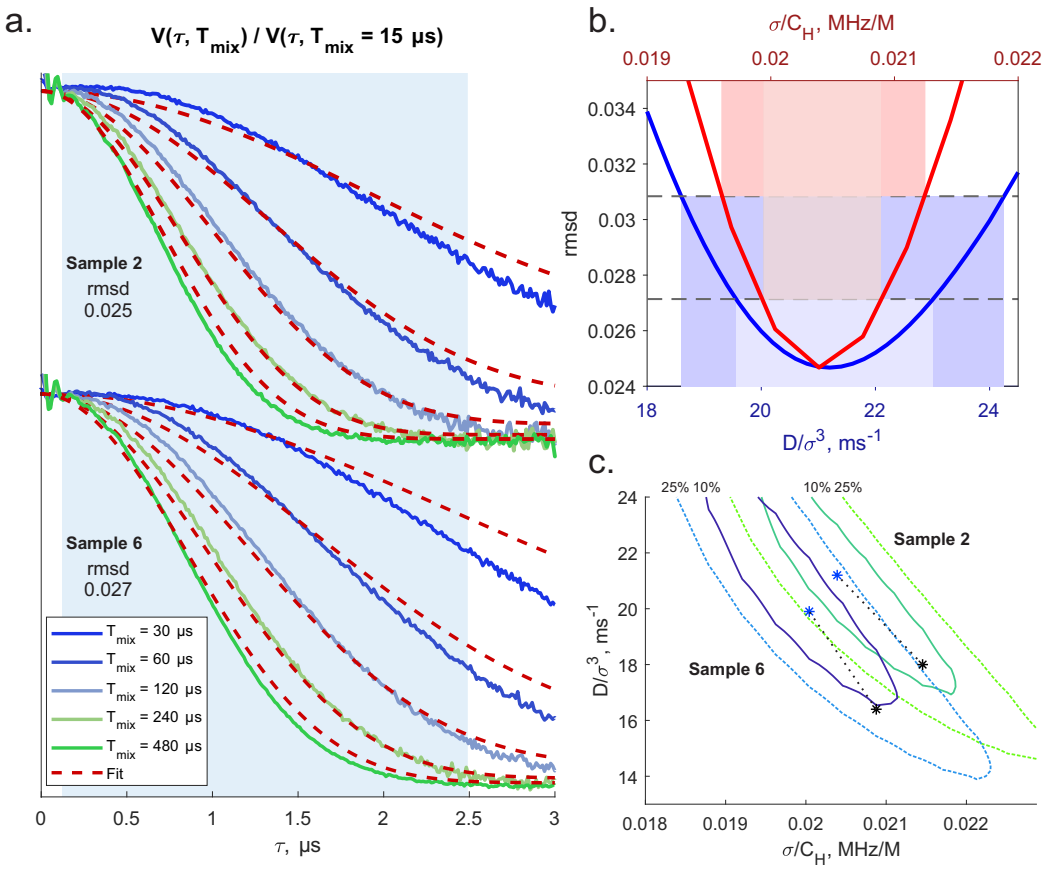

Figure S5: Overview of fitting results: (a) Series of RIDME traces measured for samples 2 and 6 divided by those with $T_{mix} = 15\ \mu s$. Best fits (dashed curves). Highlighted in light blue is the region of time domain which was included in the calculation of rmsd. (b) One-dimensional scans of the rmsd surface along fitting parameters: D/σ^3 (blue curve) and σ/C_H (red curve) corresponding to the sample 2. Coloured areas show the apparent uncertainties with respect to 10%- and 25% of the minimal rmsd. (c) Maps of two-parametric rmsd scans: minimal rmsd with $T_{mix}^{ref} = 15\ \mu s$ (blue stars), minimal rmsd with $T_{mix}^{ref} = 30\ \mu s$ (black stars, see the main text), 10%-increase (solid lines) and 25%-increase (dashed lines) of rmsd.

References

[1] M. Abramowitz, I. A. Stegun, Handbook of Mathematical Functions with Formulas, Graphs, and Mathematical Tables, Dover, New York, ninth dover printing, tenth gpo printing edition, 1964.

[2] S. Milikisyants, F. Scarpelli, M. G. Finiguerra, M. Ubbink, M. Huber, A pulsed EPR method to determine distances between paramagnetic centers with strong spectral anisotropy and radicals: The dead-time free RIDME sequence, J. Magn. Reson. 201 (2009) 48–56.

[3] L. Kulik, S. Dzuba, I. Grigoryev, Y. Tsvetkov, Electron dipole–dipole interaction in ESEEM of nitroxide biradicals, Chem. Phys. Lett. 343 (2001) 315–324.